HIV-1 Reverse Transcriptase Resistance to Nonnucleoside Inhibitors†

Rebecca A. Spence,‡ Karen S. Anderson,*,§ and Kenneth A. Johnson*,‡

Department of Biochemistry and Molecular Biology, 106 Althouse Laboratory, The Pennsylvania State University, University Park, Pennsylvania 16802, and Department of Pharmacology, Yale University Medical School, 333 Cedar Street, New Haven, Connecticut 06520

Received August 30, 1995; Revised Manuscript Received November 22, 1995⊗

ABSTRACT: The parameters governing the polymerization mechanism of reverse transcriptase containing the tyrosine to cysteine mutation at position 181 (Y181C) were determined using pre-steady-state techniques. The pathway for single nucleotide incorporation catalyzed by Y181C is similar to that determined for wild-type RT where a rate-limiting conformational change precedes fast chemistry and is followed by slow steady-state release of the primer/template. The Y181C mutant enzyme binds a 25/45-mer duplex DNA tightly with a K_d of 11 nM. However, the Y181C mutation weakens the nucleotide affinity 2−3-fold relative to the wild-type complex. We also determined the parameters governing the mechanism of nonnucleoside inhibitor resistance with Y181C. The K_d value of Nevirapine with the mutant E·DNA complex increased approximately 500-fold. The decreased affinity of Nevirapine for the mutant enzyme is a consequence of a faster inhibitor dissociation rate from the enzyme complex of Y181C relative to that of the wild-type. The E·DNA complex of Y181C may be saturated with Nevirapine, and the I·E·DNA complex is capable of a maximum incorporation rate of 0.1 s^{-1} (a 10-fold faster rate than that of the wild-type I·E·DNA complex). The overall two-step binding of nucleotide to Y181C in the presence of Nevirapine remains unaffected.

HIV-1[1] reverse transcriptase (RT) is responsible for the replication of single-stranded viral RNA into double-stranded DNA prior to integration into the genome of the human host (Barre-Sinnoussi et al., 1983; Popovic et al., 1984; Larder et al., 1989b). RT has become the main target of antiviral therapeutic agents in the treatment of AIDS (De Clercq, 1994; Mitsuya et al., 1990; Hirsch & D'Aquila, 1993; Richman, 1993). In addition to the clinically approved nucleotide analog inhibitors (i.e., AZT, ddC), a class of nonnucleoside inhibitors has emerged. These inhibitors include tetrahydroimadazo (4,5,1-j,k)-1,4-benzodiazepin-2(1H)-one and -thione (TIBO) derivatives (Pauwels et al., 1990), pyridinones (Goldman et al., 1991), 11-cyclopropyl-5,11-dihydro-4-methyl-6H-dipyrido(3,2-b:2′,3′-e)-1,4-diazepin-6-one (BI-RG-587 or Nevirapine) derivatives (Merluzzi et al., 1990), α-anilinophenylacetamide (α-APA) (Pauwels et al., 1993), and 1-((2-hydroxyethoxy)methyl)-6-(phenylthio)thymine (HEPT) derivatives (Baba et al., 1989). Nonnucleoside inhibitors specifically inhibit HIV-1 RT at low concentrations offering a potential treatment for AIDS therapy. However, as in the case of the nucleoside analogs (Larder et al., 1989a; Larder & Kemp, 1989), long term inhibition of RT by the nonnucleoside compounds is limited by the high mutational frequency of the virus, allowing drug-resistant forms to accumulate (Mellors et al., 1992; Nunberg et al., 1991; Richman et al., 1991; Mellors et al., 1993; Richman et al., 1994; Goldman et al., 1993).

The first high-resolution (3.5 Å) crystal structure of RT was determined with the enzyme bound to the nonnucleoside inhibitor Nevirapine (Kohlstaedt et al., 1992). Nevirapine was shown to bind in a hydrophobic region of the p66 subunit of RT near but not overlapping the catalytic active site. It has been proposed that the structurally diverse nonnucleoside inhibitors bind in the same region of the enzyme based on competitive binding studies (Goldman et al., 1991; Nunberg et al., 1991; Wu et al., 1991; Dueweke et al., 1992) and the observed cross-resistance of the nonnucleoside inhibitors (Mellors et al., 1992; Nunberg et al., 1991; Richman et al., 1991; Balzarini et al., 1993; Mellors et al., 1993). Recently, several crystal structures of RT with different nonnucleoside inhibitors bound (HEPT, α-APA, and TIBO derivatives) confirm that the inhibitor binding sites overlap (Ren et al., 1995; Ding et al., 1995a,b).

The predominant source of nonnucleoside inhibitor resistance is a point mutation of RT generated in the vicinity of the inhibitor binding site (Tantillo et al., 1994). One of the most common RT point mutations found *in vivo* (De Clercq, 1994) upon prolonged use of Nevirapine, as well as other nonnucleoside inhibitors, is the alteration of tyrosine to cysteine at position 181. Nevirapine contacts both Y181 and Y188 of the p66 subunit of RT (Kohlstaedt et al., 1992; Ren et al., 1995). These two aromatic amino acid residues are essential for the high inhibitory activity of most nonnucleoside inhibitors. Substitution of HIV-1 RT Y181and Y188 with the analogous HIV-2 RT amino acids (Ile and Leu, respectively) severely reduces the inhibitory action of the nonnucleoside inhibitors (Shih et al., 1991; Condra et al., 1992). It has been suggested that the aromatic nature of these

† This work was supported by grants from the National Institutes of Health, GM44613 (K.A.J.) and NIH GM49551 (K.S.A.).

* Corresponding authors.
‡ The Pennsylvania State University.
§ Yale University Medical School.

⊗ Abstract published in *Advance ACS Abstracts,* January 1, 1996.

[1] Abbreviations: HIV-1, human immunodeficiency virus-type 1; RT, reverse transcriptase; AIDS, acquired immunodeficiency syndrome; AZT, 3′-azido-3′-deoxythymidine; ddC, dideoxycytosine 5′-triphosphate; SDS−PAGE, sodium dodecyl sulfate−polyacrylamide gel electrophoresis; dATP, deoxyadenosine 5′-triphosphate; EDTA, ethylenediaminetetraacetic acid disodium salt; Tris, tris(hydroxymethyl)-aminomethane.

0006-2960/96/0435-1054$12.00/0

tyrosines provides the favorable hydrophobic interactions required for inhibitor binding.

We have defined previously the complete polymerization mechanism of wild-type RT (Kati et al., 1992) by pre-steady-state techniques. We have also shown that in the presence of nonnucleoside inhibitors (Nevirapine and two TIBO derivatives) the conformational change of the enzyme after nucleotide binding is no longer the rate-limiting step in the mechanism. Tight nucleotide binding to the inhibited E·DNA (I·E·DNA) complex leads to rate-limiting chemical incorporation allowing the two-step nucleotide binding to come to equilibrium (Rittinger et al., 1995; Spence et al., 1995). We now extend this work in order to understand more completely the role of Y181 in the polymerization mechanism and the nonnucleoside inhibitor resistance of RT. This report details the pre-steady-state characterization of RT containing the tyrosine to cysteine mutation at position 181 (Y181C) and the implications that this mutation has on the polymerization mechanism of RT. Furthermore, we describe the effect of the Y181C mutation on Nevirapine binding and release as well as nucleotide equilibrium and catalytic turnover of the I·E·DNA complex. The biochemical analysis of the Y181C mutant presented here provides insight into the design of potentially more potent drugs and/or combination therapies for the treatment of AIDS.

MATERIALS AND METHODS

RT,p51(Y181C) Construction. Clones of the HIV-1 reverse transcriptase subunits p66(Y181C) and p51(WT) in *Escherichia coli* strain TG-1 were provided by Roger Goody (Maass et al., 1993). Because the p51 subunit is believed to be a proteolytic cleavage product of the p66 subunit (Lightfoote et al., 1986), both subunits of RT contain the Y181C mutation in the physiologically relevant HIV-1 RT heterodimer. The construct encoding the p51 subunit containing the Y181C mutation was created using conventional molecular biology techniques (Ausubel et al., 1992). The plasmid pKK233-2 (Amann & Brosius, 1985) containing the sequence for the HIV-1 RT p66 subunit with a one base mutation (TAT→TGT, producing the amino acid change of Y181C in the expressed protein) was digested with *Bam*H1 and *Kpn*1. The DNA fragment corresponding to the p51 subunit was then isolated from the fragment corresponding to the RNase H domain. A separate digestion was performed on an identical vector containing the sequence for the wild-type p51 subunit. The mutated p51 fragment was ligated into the isolated vector that had previously contained the p51 wild-type subunit sequence. The newly constructed vector, containing the relevant base mutation in the p51 subunit sequence, was used to transform JM109 competent cells (Clontech, Palo Alto, CA). The extracted plasmid DNA from the JM109 cells was then used to transform the *E. coli* cell line CGSC 6662, pDMI.1 (Muller et al., 1989) for expression and purification of the p51(Y181C) subunit. The previously prepared *E. coli* cell line, CGSC 6662, pDMI.1 containing the plasmid encoding the p66(Y181C) subunit, was provided by R. Goody.

Protein Expression and Purification. Transformed cells producing the mutant subunits were grown separately in Luria Broth media supplemented with ampicillin (0.1 mg/mL) at 37 °C. The cells were induced at $A_{595} = 0.65-0.70$ by the addition of 0.5 mM isopropyl β-D-thiogalactopyranoside (IPTG). The cells were then grown for 11 h at 37 °C and harvested by centrifugation. The crude cell lysates were analyzed after induction by SDS−PAGE stained with Coomassie Blue. The intensity of the bands corresponding to the p51(Y181C) and the p66(Y181C) subunits showed that the p51(Y181C) subunit was more strongly induced than the p66(Y181C) subunit. The cell pastes were combined in a ratio of 1:1.2 by weight for the small and large subunit, respectively, in order to obtain equal amounts of the subunits in the subsequent purification steps.

Purification of Y181C was based on a modification of the procedure followed by Kati et al. (1992). The purification procedure was performed at 4 °C and is briefly described below. The cells (12 g) were resuspended in buffer A (50 mM Tris-HCl, pH 8.0, 50 mM NaCl, 2 mM EDTA, 1 mM phenylmethanesulfonyl fluoride, 10% glycerol, 0.01% Triton-X, and 1 mM dithiothreitol) to a final volume of 120 mL. The cells were lysed by the addition of lysozyme (0.5 mg/mL) followed by mild sonication. The cell extract was centrifuged, and polyethylenimine (PEI) was added to the supernatant to a final concentration of 0.3% in order to precipitate the nucleic acids. RT remained in the supernatant after centrifugation of the PEI extract. The proteins were precipitated by ammonium sulfate fractionation (0−60%). The pellets obtained after centrifugation of the ammonium sulfate fraction were resuspended in buffer A. The suspension was dialyzed in buffer A overnight and loaded onto a phosphocellulose (Whatman, P-11) column equilibrated in buffer A. A linear gradient of 50−700 mM NaCl was run to elute RT from the resin. The fractions enriched in RT, as observed by SDS−PAGE, were pooled and dialyzed in buffer A overnight. The dialysate was loaded onto a Q-Sepharose (Sigma) column equilibrated in buffer A. RT did not bind to the resin and eluted to near homogeneity after washing the column with buffer A. The final pooled fractions were concentrated, aliquoted, and flash frozen in liquid N_2; the protein was stored at −80 °C. Densitometry of the final Coomassie Blue stained polyacrylamide denaturing gel revealed Y181C >97% pure, and the molar ratio of the subunits was 1:1.1 for the small and large subunits, respectively. The enzyme concentration was determined by absorbance at 280 nm using extinction coefficients 134 870 M^{-1} cm^{-1} for p66(Y181C) and 122 780 M^{-1} cm^{-1} for p51(Y181C). Enzyme concentration was corrected based on the active site titrations as described below.

Synthetic Oligonucleotides. All experiments were performed with a sequence-specific DNA duplex 25/45-mer (Kati et al., 1992) in which the next correct base for incorporation was dATP. These oligonucleotides were synthesized by Midland Certified Reagent Co. (Midland, TX) or Integrated DNA Technologies, Inc. (Coralville, IA) and further purified by denaturing polyacrylamide gel electrophoresis. Concentrations of the oligonucleotides were estimated by UV absorbance at 260 nm using the following calculated extinction coefficients: 25-mer, $\epsilon = 249\,040$ M^{-1} cm^{-1} 45-mer, $\epsilon = 491\,960$ M^{-1} cm^{-1}. The 25-mer and 45-mer were annealed by mixing approximately equimolar amounts at ∼85 °C followed by cooling to room temperature over a period of 1.5 h.

Materials. The dATP used in these experiments was purchased from Pharmacia LKB Biotechnology, Inc. (Uppsala, Sweden). [γ-^{32}P]ATP (>4500 Ci/mmol) was purchased from ICN Biomedicals, Inc. (Costa Mesa, CA). T4 poly-

nucleotide kinase and kinase buffer were from New England Biolabs (Beverly, MA) or GIBCO BRL, Life Technologies, Inc. (Gaithersburg, MD). Bio-Spin-30 columns were obtained from Bio-Rad Laboratories, Inc. (Hercules, CA).

5′-^{32}P Labeling of Primer, 25-Mer. Before annealing, the primer was 5′-radiolabeled with T4 polynucleotide kinase and [γ-^{32}P]ATP following the procedure of Maniatis et al. (1989). The kinase was denatured after 1 h by placing the reaction at 90 °C for 5−10 min. Contaminating nucleotides were removed from the labeled primer using a Bio-Spin-30 column.

Rapid Quench Experiments. Rapid quench experiments were carried out in an apparatus designed by Johnson (1986) and built by KinTek Corporation (State College, PA). Typically, the experiments were carried out by allowing RT and duplex DNA to preincubate in reaction buffer (50 mM Tris-HCl, 50 mM NaCl, pH 8.0) either in the presence or absence of 10 mM $MgCl_2$. An aliquot of this solution (15 μL) was then rapidly mixed with an equal volume of substrate and allowed to react for the indicated times. The reaction was terminated by quenching with approximately 80 μL of 0.5 M EDTA, pH 8.0. The buffer for nucleotide substrate is as stated above; however, the required Mg^{2+} was always present with the nucleotide prior to mixing with the E·DNA complex in a concentration sufficient to allow for a final concentration of 10 mM $MgCl_2$. The nonnucleoside inhibitor was stored in dimethylsulfoxide (DMSO) at −20 °C. The final concentrations of DMSO were always <3% and had no effect on the measured rates. All reactions were performed at 37 °C. Unless noted otherwise, all concentrations quoted in the text refer to concentrations during the polymerization reaction.

Product Analysis. Single nucleotide incorporation was monitored by extension of 5′-^{32}P-25-mer to 26-mer. The products were resolved on a denaturing polyacrylamide gel (16%), and the dried gel was scanned to visualize the bands using a Betascope 603 blot analyzer (Betagen, Waltham, MA) for quantitation.

Data Analysis. Data were fit by nonlinear regression using the program GraFit (Erithacus Software). The pre-steady-state burst experiments were fit to the burst equation: $y = A[1 - \exp(-k_1 t) + mt)$, where A represents the burst amplitude, k_1 the burst rate, and m the slope. The steady-state rate is calculated by dividing the slope by the concentration of total active enzyme. The equilibrium dissociation constants for the I·E·DNA complex were defined by quadratic fits to the data: $y = E_o - 0.5\{(K_d + E_o + I_o) - [(K_d + E_o + I_o)^2 - 4E_oI_o]^{1/2}\}$, where y represents the E·DNA complex, E_o is the total enzyme concentration, I_o is the total inhibitor concentration, and K_d is the equilibrium dissociation constant for the nonnucleoside inhibitor.

Enzyme Active Site Titration. The number of RT active sites was determined by an active site titration as previously described (Kati et al., 1992). RT was preincubated with increasing concentrations of 5′-^{32}P-labeled 25/45-mer for 5−10 min at 37 °C in reaction buffer. An aliquot of this solution was then rapidly mixed with an equal volume of dATP and allowed to react for the indicated times. The reaction was terminated by quenching with ∼80 μL of 0.5 M EDTA, pH 8.0. The amplitudes were obtained by fitting each time course to the burst equation. The amplitudes were then plotted as a function of the DNA concentrations, and the data were fit to a quadratic equation.

The maximum amplitude obtained by the mutant E·DNA complex (see Figure 1) was approximately 40% of what might be expected on the basis of the absorbance measurements used to determine the protein concentration. It has been suggested that RT may bind to the blunt-end of the primer/template and, therefore, appear inactive. We have determined that RT binds approximately 10-fold weaker to the blunt end of our primer/template relative to the staggered end of the duplex DNA (G. Jin and K. A. Johnson, unpublished observations). This blunt-end binding is too weak to account for the low amplitude in our active site titration. Moreover, we have observed variable amplitudes as high as 80% in different enzyme preparations. The active site titrations in this report are similar to those reported in studies with wild-type RT in the absence (Kati et al., 1992) and in the presence of nonnucleoside inhibitors (Spence et al., 1995), and the amplitudes and rates under these assay conditions are consistent. Further experiments are currently underway to resolve the basis for the apparent low amplitude of the active site titration.

Determination of the Inhibitor Binding Rate. The apparent binding rate of Nevirapine to the E·DNA complex was determined by means of a rapid quench-flow method entailing three sequential mixing events. First, a solution containing the E·DNA complex was rapidly mixed with the inhibitor and incubated for a specified time. Second, the next correct nucleotide for incorporation, dATP, was added to allow polymerization catalyzed by uninhibited enzyme. Third, the polymerization reaction was stopped by mixing with 100 μL of 0.5 M EDTA (pH 8.0) after 200 ms, a time sufficient to complete one enzyme turnover of the E·DNA complex. The reported concentrations of RT, DNA, and Nevirapine are the concentrations after 1:1 mixing; the reported concentration of dATP is the final concentration after mixing 1:2 with the E·DNA and inhibitor solutions. The product DNA concentrations were normalized by the maximum amount of turnover seen in 200 ms (the amount of product formed in 200 ms in the absence of inhibitor). The data were fit to a single-exponential decay plus a constant: $y = A \exp(-k_{obs} t) + C$, where A is equal to the difference in the burst amplitudes of polymerization catalyzed by E·DNA and E·DNA partially saturated with inhibitor. The rate constant, k_{obs}, is the observed rate of inhibitor binding, and C reflects the burst amplitude of the equilibrium obtained between the inhibitor and the E·DNA complex.

Maximum Catalytic Rate in the Presence of Saturating Amounts of Inhibitor. RT and duplex DNA were first preincubated for 10−15 min followed by the addition of saturating amounts (>6K_d) of Nevirapine. After the second incubation period of 10−15 min, the reaction was initiated by mixing equal volumes of Mg^{2+}·dATP with the pre-formed I·E·DNA complex. The reaction was then quenched with 0.5 M EDTA, pH 8.0, at the indicated times. A single-exponential equation was used to determine the single incorporation rates for each dATP concentration (Figure 5A). The single turnover rates of the I·E·DNA complex were plotted as a function of the dATP concentration. The data (Figure 5B) were fit to a hyperbolic function which defined the maximum rate of incorporation and apparent K_d of dATP in the presence of saturating amounts of inhibitor.

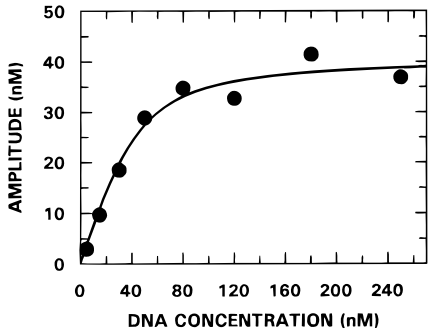

FIGURE 1: Active site titration of Y181C with 25/45-mer duplex DNA. Y181C (100 nM as determined by absorbance measurements at 280 nm) and increasing concentrations of 5′-^{32}P-labeled 25/45-mer were incubated for 5−10 min at 37 °C in reaction buffer containing 10 mM $MgCl_2$. The E·DNA complex was rapidly mixed with 100 μM Mg^{2+}·dATP and quenched with 0.5 M EDTA, pH 8.0. The amplitudes were obtained by fitting each time course to the burst equation (see Materials and Methods). The amplitudes (●) were plotted as a function of the DNA concentrations. The solid line represents the data fit to a quadratic equation: $[E{\cdot}DNA] = 0.5\{(K_d + E_o + D_o) - [(K_d + E_o + D_o)^2 - 4E_oD_o]^{0.5}\}$. The fit of the data yielded a K_d value for the E·DNA complex of 11.1 ± 3.8 nM. The maximum amplitude, 40.9 ± 2.2 nM, was used to establish the active site concentration for all other experiments reported in this paper.

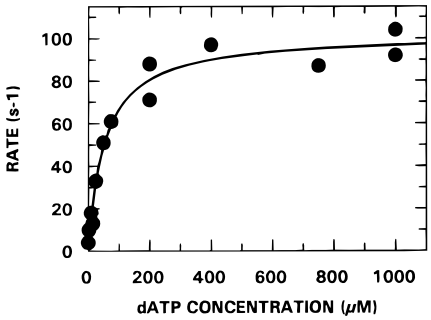

FIGURE 2: Pre-steady-state burst rate dependence on dATP concentration. Y181C (50 nM) and 5′-^{32}P-labeled 25/45-mer (100 nM) were preincubated in reaction buffer containing 10 mM $MgCl_2$ for 5−10 min at 37 °C. The reaction was initiated by mixing equal volumes of Mg^{2+}·dATP and quenched with EDTA. Each burst phase was fit to a single exponential. The first turnover rates (●) obtained from these fits were plotted as a function of dATP concentration. The rate data were fit to a hyperbolic function (solid line) that yielded a K_d of 53.9 ± 9.0 μM for dATP and a maximum incorporation rate of 102.1 ± 4.0 s^{-1}.

RESULTS

Single nucleotide incorporation experiments with HIV-1 Y181C were performed to compare the kinetics of the mutant enzyme to the wild-type enzyme. The mutant E·DNA complex was rapidly mixed with a saturating concentration of dATP, the next correct nucleotide for incorporation into the 25/45-mer DNA, followed by quenching with 0.5 M EDTA, pH 8.0. Analysis of the 26-mer product DNA showed a burst phase of incorporation followed by a slow, linear phase (data not shown). The burst phase corresponded to the first turnover of the enzyme. The slope of the slow linear phase divided by the active enzyme concentration determined the rate constant for release of the primer/template from the enzyme following single nucleotide incorporation (Kati et al., 1992; Reardon & Miller, 1990). This initial experiment indicated that both the burst and steady-state rates were of similar magnitude relative to that of the wild type enzyme (Kati et al., 1992).

Active Site Titration of Y181C with 25/45-mer DNA. The biphasic nature of the single nucleotide incorporation reaction for Y181C suggests that the mutant enzyme follows a similar kinetic mechanism relative to wild type, where fast nucleotide incorporation is followed by a slow steady-state release of the duplex DNA from the enzyme. Because catalysis is much faster than the release of DNA from the enzyme, the amplitude of the burst phase in a single nucleotide incorporation reaction is a direct measurement of the amount of E·DNA complex proceeding to the first turnover. The relationship between the amplitude and the concentration of the E·DNA complex made it possible to examine the number of enzyme active sites and determine the equilibrium dissociation constant of DNA from Y181C. Single nucleotide incorporation experiments were performed where increasing concentrations of radiolabeled 25/45-mer were incubated with a fixed concentration of Y181C prior to mixing with the next correct nucleotide. Figure 1 shows the DNA concentration dependence of the burst amplitude. The data were fit to obtain a K_d value of 11.1 ± 3.8 nM, which is similar to that seen for the wild-type RT ($K_{d,wt}$ = 5 nM; Kati et al., 1992). Therefore, the Y181C mutation has no significant effect on DNA binding. The Y181C concentration was defined on the basis of the active site titration described in Figure 1 and is comparable to that reported for wild-type RT. Y181C concentrations reported for all subsequent experiments are active site concentrations.

Recent work has shown that incubation of the required Mg^{2+} ion with the wild-type E·DNA complex prior to reaction with the next correct nucleotide results in a significant (3−5-fold) increase in the burst rate (Spence et al., 1995). The preincubation of the metal ion with the wild-type E·DNA complex had no significant affect on either the maximum amplitude or the K_d of the E·DNA complex.[2] We performed an active site titration of Y181C analogous to Figure 1 where the Mg^{2+} ion required for catalysis was added only to the nucleotide solution prior to the polymerization reaction. The results of this experiment were identical to the results seen in Figure 1. Therefore, these data show that Y181C forms a tight complex with duplex DNA in the presence or absence of Mg^{2+}.

Incorporation of the Next Correct Nucleotide, dATP. Tyrosine 181 is near the polymerization active site and potentially may interact with the incoming nucleotide. We wanted to determine if the affinity of the incoming nucleotide for the E·DNA complex was affected by the Y181C mutation. Single turnover experiments were done in which the pre-formed Mg^{2+}·E·DNA complex was rapidly mixed with increasing concentrations of dATP. The burst phases were fit to single-exponential equations in order to obtain the first turnover rate at each nucleotide concentration. Figure 2 shows the dATP concentration dependence of the burst rate catalyzed by the Mg^{2+}·E·DNA complex. In order to compare directly the mutant enzyme with the wild-type enzyme, experiments with wild-type RT were performed analogous to those described in Figure 2. The pre-steady-state burst rate dependence on nucleotide concentration for both the wild-type and Y181C RT enzymes are reported in

[2] Other laboratories have observed a significant increase in the burst amplitude upon preincubation of the E·DNA complex with metal ions (Hsieh et al., 1993; Patel et al., 1995). However, our results are in agreement with those of Kruhoffer et al. (1993), whereby DNA binding to RT is only marginally, if at all, affected by Mg^{2+} ions.

Table 1: Kinetic Properties of Wild-Type RT and Y181C

	Mg^{2+}·E·DNA[a]		E·DNA[b]	
	WT	Y181C	WT	Y181C
K_d (dATP μM)	26.1 ± 10.6	53.9 ± 9.0	3.8 ± 0.7[c]	12.5 ± 4.2
max. incorp. rates^{-1}	95.4 ± 10.2	102.1 ± 4.0	20.7 ± 1.2[c]	16.8 ± 1.1
K_d (Nevirapine μM)	0.025 ± 0.01[d]	11.7 ± 4.3	0.019 ± 0.004[d]	2.5 ± 1.3

[a] Mg^{2+} was preincubated with the E·DNA solution prior to nucleotide incorporation. [b] Mg^{2+} was added only to the nucleotide solution to initiate the reaction. [c] Previously determined values by Kati et al. (1992): K_d, dATP = 4.0 ± 0.4 μM and maximum rate, 33 ± 1.2 s^{-1}. [d] Previously determined values by Spence et al. (1995).

Table 1. Table 1 shows that the nucleotide interaction is weakened 2−3-fold with the Y181C E·DNA complex relative to wild-type RT. Therefore, the Y181C mutation slightly alters the incoming nucleotide interactions with the protein complex.

A 5-fold increase in the maximum burst rate was observed for both wild-type RT and Y181C when Mg^{2+} was preincubated with the E·DNA complex. As stated above, the increased burst rate with the Mg^{2+}·E·DNA complex has been observed previously (Spence et al., 1995). The basis for the Mg^{2+} dependence is still under investigation (see Discussion). In addition, for both the wild-type and the mutant enzyme the nucleotide had approximately 5-fold weaker affinity when the E·DNA complex was incubated with Mg^{2+} prior to starting the reaction by the addition of nucleotide.

Steady-state experiments were performed to determine the rate of DNA dissociation from the mutant enzyme in comparison to the wild type. 5′-^{32}P-labeled 25/45-mer was added in large excess to Y181C and incubated at 37 °C prior to mixing with Mg^{2+}·dATP to initiate polymerization. The reaction was quenched manually with 0.5 M EDTA, pH 8.0, at times ranging from 4 to 30 s (data not shown). A steady-state rate of 0.12 ± 0.02 s^{-1} was measured. The dissociation rate of DNA from Y181C is not significantly different from the wild-type steady-state rate of 0.18 s^{-1} (Kati et al., 1992).

The parameters governing DNA binding and nucleotide incorporation have been examined for Y181C. The Y181C results relative to wild-type RT indicate that the mutant enzyme does not alter the kinetic mechanism for single nucleotide incorporation. We have shown that the Y181C mutation does not significantly affect DNA binding and dissociation. This amino acid change does, however, play a small role in nucleotide interactions with the E·DNA complex. The affinity of the incoming nucleotide in the ground state is decreased approximately 3-fold for the mutant E·DNA complex relative to wild-type complex. The distance of Y181 from the nucleotide site suggests that the effect of the Y181C mutation may be due to an indirect effect on protein structure which is propagated to the nucleotide site. Once Y181C is saturated with nucleotide, the rate of incorporation is similar to that of the wild type. We suggest that Y181C follows the same mechanistic pathway previously determined for wild-type RT (Kati et al., 1992).

Y181C in the Presence of a Nonnucleoside Inhibitor. Several laboratories have found that the tyrosine to cysteine mutation at position 181 renders RT resistant to most nonnucleoside inhibitors both *in vivo* and *in vitro*. The cause of this resistance is proposed to be due to the loss of the aromatic side chain which provides necessary hydrophobic stacking interactions between the enzyme and inhibitor (Sardana et al., 1992). We have gained further insight into nonnucleoside inhibitor resistance of Y181C by studying the polymerization mechanism of this mutant in the presence of a nonnucleoside inhibitor using pre-steady-state techniques.

Single Nucleotide Incorporation in the Presence of a Nonnucleoside Inhibitor. Our report describing the mechanism of wild-type RT in the presence of nonnucleoside inhibitors (Spence et al., 1995) supports a slow equilibrium between the E·DNA complex and the inhibitor. Titrating the E·DNA complex with increasing amounts of inhibitor prior to single nucleotide incorporation led to a monotonic reduction in the amplitude of the burst phase of polymerization. The amplitude of the burst phase represents the amount of uninhibited E·DNA proceeding to nucleotide incorporation in the first turnover. The reduction of the burst amplitude without an effect on the rate suggests that the inhibitor dissociates from the I·E·DNA complex slowly relative to the rate of the uninhibited polymerization reaction. Our initial goal was to determine if the mutant E·DNA complex could be saturated with the nonnucleoside inhibitor, Nevirapine, and if there still exists a slow equilibrium between the free and inhibited E·DNA complexes similar to that seen for the wild type. E·DNA was titrated with Nevirapine prior to rapid mixing with the next correct nucleotide, and after various times the reaction was quenched with EDTA (Figure 3A). The rate of the burst phase did not vary significantly between the different reactions, suggesting that the fast rate of incorporation was due to the first turnover of uninhibited E·DNA. Therefore, the observed reduction in amplitude of the burst phase of polymerization was due to the amount of inhibitor-bound E·DNA complex. The results of the experiments described in Figure 3A suggest that, as seen in the case of wild type, the inhibitor dissociates from the mutant I·E·DNA complex slowly relative to the rate of nucleotide incorporation by uninhibited E·DNA. The direct measurement of the I·E·DNA complex allows us to determine the equilibrium dissociation constant of the inhibitor binding to the E·DNA complex. In Figure 3B the amplitudes of the burst phases are plotted as a function of Nevirapine concentration. The data are fit to a quadratic equation to yield a K_d of 11.7 ± 4.3 μM. In comparison to the wild-type enzyme (Spence et al., 1995), the affinity of Nevirapine for Y181C has decreased approximately 500-fold. Preliminary studies of wild-type RT with a DNA/RNA primer/template in the presence of Nevirapine show similar results. Further studies are in progress to determine the kinetic parameters of the RNA-directed polymerization in the presence of nonnucleoside inhibitors.

We previously observed a decreased affinity of the nonnucleoside inhibitors for the wild-type E·DNA complex when Mg^{2+} was preincubated with the E·DNA complex prior to the addition of Nevirapine (Spence et al., 1995). We concluded that there exists an interaction between the nonnucleoside inhibitor binding site and the metal ion binding

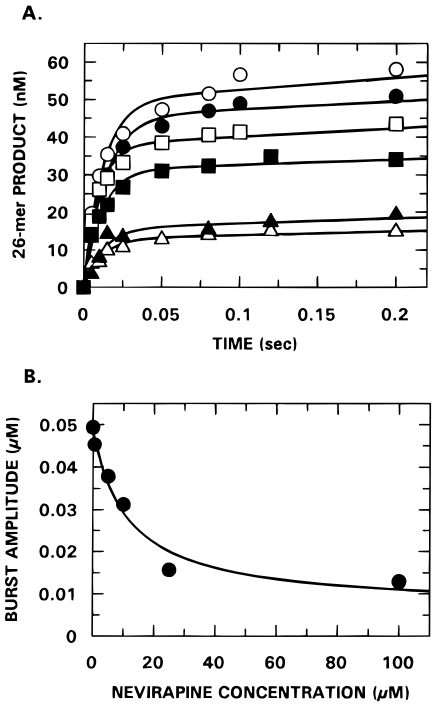

FIGURE 3: Single nucleotide incorporation in the presence of Nevirapine. (A) Y181C (50 nM), 5′-^{32}P-labeled 25/45-mer DNA (100 nM), and Nevirapine were preincubated for 15−20 min at 37 °C in reaction buffer containing 10 mM $MgCl_2$. The partially saturated E·DNA complex was rapidly mixed with an equal volume of 150 μM dATP (10 mM $MgCl_2$), and the reactions were quenched with EDTA at the indicated times. The Nevirapine concentrations were 0 (○), 0.5 (●), 5.0 (□), 10.0 (■), 25.0 (▲), and 100 (△) μM. The concentrations reported are the final concentrations after 1:1 mixing except for Nevirapine. The Nevirapine concentrations are those of the inhibitor in the initial E·DNA solution where equilibrium is established. The individual time courses were fit to the burst equation (see Materials and Methods). (B) The amplitudes of the burst phases (●) were plotted against the Nevirapine concentrations. The data were fit to a quadratic equation (solid line) that defined a K_d value of 11.7 ± 4.3 μM.

site at the catalytic center of RT. Crystallographic data have shown that Y181 is rotated toward the catalytic center when a nonnucleoside inhibitor is bound to RT (Rodgers et al., 1995). Accordingly, the Y181C mutation could affect the communication between the inhibitor and nucleotide sites. Experiments analogous to those described in Figure 3 were performed, where Mg^{2+} was contained only in the nucleotide solution prior to mixing with the mutant E·DNA to initiate the polymerization reaction. The K_d value of 2.5 ± 1.3 μM was determined (data not shown). The K_d values of Nevirapine indicate that the nonnucleoside inhibitor binds tighter (∼6-fold) to the E·DNA complex relative to the Mg^{2+}·E·DNA complex. Similar results were obtained for the wild-type E·DNA complex with two TIBO derivatives (Spence et al., 1995). We did not measure a significant difference in Nevirapine affinity to the wild-type E·DNA complex relative to the complex preincubated with Mg^{2+} ion, although it is likely that the affinity difference exists. The extremely small K_d values for Nevirapine binding (20 nM) determined for wild-type E·DNA or Mg^{2+}·E·DNA complex made any change in affinity difficult to measure accurately. Much greater inhibitor concentrations are required to determine the K_d values of Nevirapine with Y181C. As a consequence, a significant change in Nevirapine affinity was observable for the mutant E·DNA complex relative to the

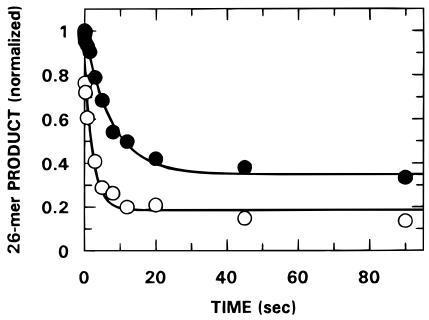

FIGURE 4: Nevirapine binding to the mutant E·DNA complex. The E·DNA complex was preformed by incubating Y181C (75 nM) and 5′-^{32}P-labeled 25/45-mer DNA (92 nM). The complex was rapidly mixed with an equal volume of 25 μM Nevirapine for the indicated times, followed by mixing with saturating concentrations of Mg^{2+}·dATP for 200 ms. The reaction was quenched with 100 μL of EDTA. The decrease in product formation with increasing incubation time of the inhibitor with the E·DNA complex reflects the binding of Nevirapine to the E·DNA complex. The enzyme was preincubated with the DNA either in the presence (●) or absence (○) of 10 mM $MgCl_2$. In either case, the final $MgCl_2$ concentration in the polymerization reaction was 10 mM. In the reaction where Mg^{2+} was present only with the nucleotide solution to initiate the reaction, the fit of the data to a single-exponential decay gave an apparent binding rate of Nevirapine to the E·DNA complex equal to 0.42 ± 0.09 s^{-1}. In the reaction where Mg^{2+} was present in all the reactant syringes, the apparent binding rate was 0.13 ± 0.01 s^{-1}.

complex preincubated with Mg^{2+} (Table 1). Therefore, the Y181C mutation still allows communication between the nonnucleoside inhibitor binding site and the metal ion binding sites of the catalytic center, leading to a reduced rate of catalysis.

Association and Dissociation Rates of Nevirapine with the E·DNA Complex. In order to fully evaluate the effect of the mutation on the equilibrium dissociation constant of Nevirapine, it was necessary to determine both the binding and dissociation rates of the inhibitor. These rate measurements were made possible by modifying our typical quench flow experiment to allow a third reactant mixing. Y181C was preincubated with the labeled 25/45-mer, either in the presence or absence of 10 mM Mg^{2+}. The pre-formed E·DNA complex was mixed with an equal volume of Nevirapine. After the indicated time, the partially saturated I·E·DNA complex was mixed with saturating concentrations of dATP. The polymerization reaction was then quenched with 0.5 M EDTA, pH 8.0, after 200 ms, allowing enough time for a single turnover of uninhibited E·DNA (Figure 4). Because the release of Nevirapine from I·E·DNA is slow relative to the rate of uninhibited polymerization, any product formed in the 200 ms mixing of dATP is due to uninhibited E·DNA. The product decrease observed with increasing incubation times of E·DNA and Nevirapine seen in Figure 4 is a result of Nevirapine binding to the enzyme complex. The data were fit to a single-exponential function yielding the apparent rate of Nevirapine binding to the E·DNA complex. The binding rate was determined from the equation, $k_{app} = k_{on}$[Nevirapine] + k_{off}, where k_{app} is the apparent binding rate of Nevirapine determined from the fitted data, and k_{on} and k_{off} are the binding and release rate of the inhibitor with the E·DNA complex, respectively. The equation was modified to limit k_{off} to be consistent with the previously determined K_d: $k_{on} = k_{app}/(K_d$ + [Nevirapine]). The apparent binding rates for 25 μM (Figure 4) and 50 μM (data not shown) Nevirapine were determined. The apparent

binding rates increased linearly with Nevirapine concentration as expected. When the required Mg^{2+} ions are added only to the nucleotide solution where they are available at the start of the polymerization reaction, the binding rate, k_{on}, of Nevirapine to the E·DNA complex is determined to be 1.55×10^4 M^{-1} s^{-1} and the k_{off} 0.039 s^{-1}. Preincubation of the metal ion with the E·DNA complex prior to the addition of nucleotide results in a k_{on} of 3.51×10^3 M^{-1} s^{-1} and k_{off} 0.041 s^{-1}. We conclude that the weaker affinity of Nevirapine for the Mg^{2+}·E·DNA complex relative to the E·DNA complex is more significantly a consequence of a slower binding rate of the inhibitor to the Mg^{2+}·E·DNA complex, rather than a faster dissociation rate. A similar observation was made for the wild-type enzyme (Spence et al., 1995).

Nucleotide Incorporation in the Presence of Saturating Nevirapine. For both wild-type and the Y181C mutant, the initial collision of dNTP with the E·DNA complex leads to ground-state binding. A subsequent conformation change of the enzyme aligns the nucleotide for catalysis. The overall nucleotide equilibrium involves a ground-state collision followed by an enzyme conformation change resulting in a tight ternary (E·DNA·dNTP) complex. The overall equilibrium for the two-step nucleotide binding prior to incorporation is 20 nM for the wild-type E·DNA complex (Rittinger et al., 1995). We have shown (Spence et al., 1995), along with Rittinger et al. (1995), that the overall equilibrium is weakened only 5-fold (K_d ~100 nM) when a nonnucleoside inhibitor is bound to the E·DNA complex. Therefore, the mechanism of catalysis by wild-type RT in the presence of nonnucleoside inhibitors supports tight nucleotide binding to the I·E·DNA complex.

We have determined that the ground-state nucleotide binding interactions are weakened with the mutant E·DNA complex relative to wild-type (Table 1). In addition, the communication between the nonnucleoside inhibitor binding site and the metal ion binding site is maintained with Y181C. We then determined the nucleotide binding affinity for the E·DNA complex saturated with Nevirapine. The pre-formed E·DNA complex was further incubated with saturating ($>6K_d$) concentrations of Nevirapine. The I·E·DNA complex was then mixed with equal volumes of Mg^{2+}·dATP and at various times polymerization was stopped with 0.5 M EDTA (pH 8.0). The single turnover rates of the inhibited complex are shown in Figure 5A as a function of dATP concentration. The dATP concentration dependence of the nucleotide incorporation rate of the fully inhibited enzyme complex is shown in Figure 5B. The apparent K_d for dATP was 114.2 ± 32.7 nM, as the result of a hyperbolic fit to the data. The nucleotide incorporation rate for the fully inhibited mutant complex reaches a maximum at 0.100 ± 0.008 s^{-1}. The nucleotide K_d for the wild-type I·E·DNA complex was reported as an upper limit of 100 nM. Therefore, the overall, two-step nucleotide equilibrium is not affected significantly by the Y181C mutation. In contrast, the nucleotide incorporation rate of the I·E·DNA complex is approximately 10 times faster than the polymerization rate of the wild-type I·E·DNA complex (Spence et al., 1995), although it is still significantly slower than the uninhibited rate.

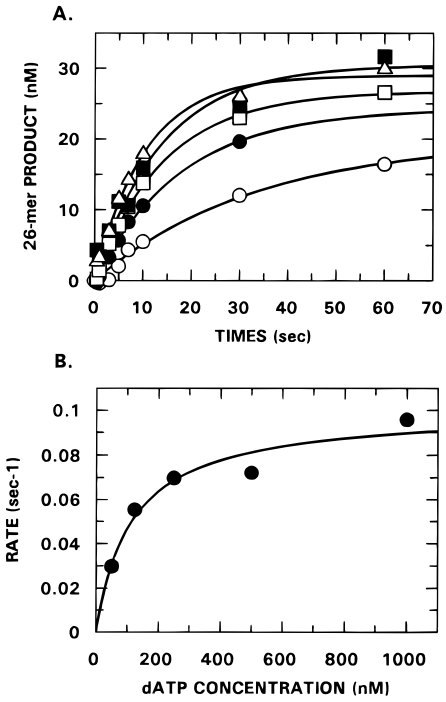

FIGURE 5: Nucleotide incorporation in the presence of saturating amounts of Nevirapine. (A) Y181C (50 nM), 5′-^{32}P-labeled 25/45-mer DNA (50 nM), and 50 μM Nevirapine were preincubated at 37 °C. The reaction was initiated by mixing equal volumes of Mg^{2+}·dATP and the E·DNA·I complex and quenched after the indicated times with EDTA. The concentrations reported are those obtained after 1:1 mixing of the enzyme solution with the nucleotide solution. Each time course was fit to a single-exponential equation (solid lines). The single turnover rates increased to a maximum value with increasing concentrations of dATP. The dATP concentrations were 0.05 (○), 0.125 (●), 0.25 (□), 0.50 (■), and 1.0 (△) μM. (B) The single incorporation rates (●) were plotted as a function of nucleotide concentrations. The data were fit to a hyperbola (solid line) that defined a K_d value of 114.2 ± 32.7 nM and a maximum rate of incorporation of 0.100 ± 0.008 s^{-1}.

DISCUSSION

The pre-steady-state studies presented here have definitively shown that the amino acid mutation of Y181C in HIV-1 RT does not significantly affect the DNA-directed polymerization mechanism relative to the wild-type enzyme. We have provided in our study an assessment of the contribution of Y181 to the elementary steps in the pathway. These data are consistent with previous steady-state data (Debyser et al., 1993; Loya et al., 1994) and cell culture assays (Richman et al., 1991) suggesting essentially unchanged replication characteristics of Y181C, although we do note a 3-fold reduction in nucleotide affinity. We have also examined this RT mutant in the presence of a nonnucleoside inhibitor to assess the role of Y181C in nonnucleoside inhibitor resistance to HIV-1 RT.

Initial single turnover experiments with Y181C displayed the same biphasic behavior as the wild-type RT indicating a fast incorporation of nucleotide followed by a slower steady-state release of DNA. Our active site experiment involved titrating increasing concentrations of duplex DNA with Y181C prior to the addition of nucleotide. The active site titration experiments allowed determination of the active site enzyme concentration and the equilibrium dissociation constant for the duplex DNA and Y181C. Our K_d value of 11 nM indicates tight binding of the mutant E·DNA complex similar to the value of 5 nM observed for the wild-type E·DNA complex. The K_d value of DNA for Y181C indicates that the Y181C mutation does not greatly influence DNA binding to the enzyme.

Tyrosine 181 is near the conserved polymerase motif of YMDD (Delarue et al., 1990) which contains two of the proposed catalytic aspartic acids residues, D185 and D186. The proximity of Y181 to the proposed catalytic site makes possible either direct or indirect interactions with the incoming nucleotide. The lack of a high-resolution crystal structure with nucleotide bound to an RT·DNA complex prevents the precise placement of Y181 during catalysis. Measurement of the equilibrium dissociation constant of the nucleotide with the E·DNA complex using Y181C has determined that the replacement of Y181 by cysteine lowers the ground-state binding affinity of the nucleotide for the E·DNA complex approximately 3-fold relative to wild type. A recent report of Mg^{2+}·dTTP modeled with wild-type HIV-1 RT complexed with duplex DNA (Patel et al., 1995) postulates potential interactions between the nucleotide and the protein. According to their analysis, Y181 does not appear to be in direct contact with the incoming nucleotide. However, it neighbors several of the amino acids that are believed to play critical roles in nucleotide binding. The decrease in affinity of the nucleotide for the mutant E·DNA complex in comparison to the wild-type complex is probably due to structural changes at the nucleotide binding site. Any changes in either backbone or side chain structure created by the mutation at position 181 may distort the precise geometry required for tight binding of the correct nucleotide. The changes conferred upon the nucleotide equilibrium when Y181 is mutated to a cysteine residue appear to be solely in the ground-state binding step and not associated with the tighter binding step concurrent with a protein conformational change as evidenced by the tight binding of dATP seen in the presence of Nevirapine.

At least two Mg^{2+} ions are proposed to participate in the catalytic mechanism of nucleotide incorporation of reverse transcriptase (Steitz, 1993). These metal ions have been observed at the active site of polymerase-β (Pelletier et al., 1994) and have been modeled into the active site of reverse transcriptase (Steitz, 1993; Patel et al., 1995). One Mg^{2+} ion that is shared between D110 and D186 chelates both the β- and γ-phosphates of the incoming base, and another Mg^{2+} ligated to D185 facilitates the attacking 3′-OH of the primer strand and stabilizes the pentacovalent α-phosphate in the transition state. Therefore, the mechanism for nucleotide incorporation depends on the precise positioning of the metal ions by the essential aspartic acids residues and neighboring amino acids. We previously observed an increase in burst rate of single nucleotide incorporation upon preincubation of the required metal ions with the E·DNA complex prior to nucleotide binding (Spence et al., 1995). An identical observation was made in experiments with the mutant enzyme. Metal binding may contribute to the rate-limiting turnover possibly by facilitating the conformational change of the protein before chemistry. Studies performed with an RNase H deficient mutant, where the specific mutation, D443N, is believed to hinder metal binding, show similar Mg^{2+} effects as wild-type RT (Z. Suo and K. A. Johnson, unpublished observations). These preliminary studies suggest that the observed Mg^{2+} effects reported in this paper are due to metal binding at the polymerase active site rather than binding at the RNase H active site. An extension of the metal studies stimulated further questions about the role of Mg^{2+} in the polymerization reaction. Experiments to evaluate the affinity of nucleotide for the E·DNA complex (both wild type and Y181C) were determined in two different ways. First, Mg^{2+} was incubated with the E·DNA complex prior to nucleotide addition. Alternatively, Mg^{2+} was added simultaneously with nucleotide to initiate the reaction. A 5-fold decrease in nucleotide affinity for the preincubated Mg^{2+}·E·DNA complex relative to the E·DNA complex was determined for both wild type and Y181C (Table 1). A conformational change of the enzyme may occur upon Mg^{2+} binding which leads to weaker ground-state binding of the nucleotide but faster catalysis. The basis for these observations remains under investigation.

Recently determined crystal structures of HIV-1 RT with four different nonnucleoside inhibitors bound (Ren et al., 1995) provide greater insight into the position of the amino acid residues surrounding the nonnucleoside inhibitor binding site relative to the apostructure. The most dramatic change between the inhibitor-bound and apostructure is the shift in the β-strands containing the proposed catalytically important aspartic acid residues (D185, D186, D110). There is significant movement of Y181, Y183, Y188, and L100 upon binding the nonnucleoside inhibitor. In contrast, similar orientations of the p66 thumb are observed in liganded and unliganded RT. These observations support our previous conclusion that the binding of nonnucleoside inhibitors alters the position of the amino acids responsible for efficient catalysis of wild-type RT. The distortion of the catalytic residues renders the chemical step of incorporation rate-limiting with no significant effect on the conformation change of the enzyme after initial nucleotide binding (Spence et al., 1995). We evaluated the polymerization mechanism of Y181C in the presence of Nevirapine. Y181C is considered resistant to Nevirapine at the nanomolar concentrations required to inhibit the wild type. However, at much higher (micromolar) concentrations of Nevirapine Y181C appears to follow the same kinetic pathway determined for the inhibited wild-type.

A reduction in the burst amplitude upon titration of the nonnucleoside inhibitor, Nevirapine, with the mutant E·DNA complex supports a slow equilibrium between the inhibitor and enzyme complex. An equilibrium dissociation constant for Nevirapine with the mutant complex was determined based on the direct correlation between the burst amplitude and the amount of I·E·DNA complex. We determined a decrease in affinity of Nevirapine for the E·DNA complex of approximately 500-fold using Y181C relative to the wild-type E·DNA complex (Figure 3; Spence et al., 1995). Measurements of the binding and dissociation rates of Nevirapine with the mutant E·DNA complex show that the substantial increase in the K_d value of Nevirapine with Y181C is more significantly a product of a faster inhibitor dissociation rate rather than a slower binding rate. The 2.2 Å resolution structure of Nevirapine-bound RT (Ren et al., 1995) shows that Y181 makes the most extensive contacts between the protein and the Nevirapine compound, presumably entirely through hydrophobic interactions. Ren et al. (1995) suggest that the mutations of RT rendering resistance to the nonnucleoside inhibitors increase the volume of the binding "pocket" allowing the inhibitor to bind to the enzyme, albeit weakly, due to the loss of specific interactions. Our results support their proposal. Nevirapine binds to Y181C with an association rate similar to that of wild-type, but the replacement of Y181 with cysteine yields the loss of substantial interactions between the protein and the inhibitor

that are necessary to bind the inhibitor tightly at this site. The dissociation rate is, therefore, faster.

Additionally, we have determined that the communication existing in the wild-type RT between the nonnucleoside inhibitor site and the catalytic active site through the metal ions remains relevant in the Y181C enzyme. The K_d value increases (12 versus 2.5 μM) when Mg^{2+} ions are bound to the mutant E·DNA complex prior to the addition of the inhibitor. The increased K_d value is defined by the slower binding rate of Nevirapine to the Mg^{2+}·E·DNA complex relative to the E·DNA complex. It has previously been proposed that several side chains, including Y181, must deform from their conformations in the apo-RT structure in order to allow the nonnucleoside inhibitor to enter the binding site (Rodgers et al., 1995; Tantillo et al., 1994; Esnouf et al., 1995). Mg^{2+} ions presumed to be coordinated to the catalytic aspartic acid residues may restrict, indirectly, the movement of these side chains on the same or neighboring β-strands, thus, hindering the binding of the inhibitor compound.

Previous studies with wild-type RT have shown that there is a slight increase in the overall two-step equilibrium dissociation constant for nucleotide when the E·DNA complex is saturated with inhibitor (Rittinger et al., 1995; Spence et al., 1995). Furthermore, the study determined that the wild-type I·E·DNA complex was capable of slow turnover. We have determined now that the next correct nucleotide binds to the mutant I·E·DNA complex with a K_d of ~115 nM. A similar value (100 nM) was reported as the upper limit for the K_d of nucleotide with the inhibited wild-type complex (Spence et al., 1995). However, we have observed a 10-fold increase in the maximum incorporation rate with the I·E·DNA using Y181C complex relative to the wild-type I·E·DNA complex. It seems probable that the bound nonnucleoside inhibitor forces the wild-type Y181 to rotate in such a manner that the precise alignment of the catalytic residues is lost. We now speculate that replacement of the tyrosine side chain at this position with a smaller cysteine residue may not require the extensive movement necessary for nonnucleoside inhibitor binding; thus, the catalytic residues are slightly closer to their proper positions for incorporation to take place.

We have considered that the slow rate of catalysis by the inhibited enzyme may be due to dissociation of the inhibitor from the I·E·DNA complex followed by rapid nucleotide incorporation catalyzed by the uninhibited E·DNA complex. Accordingly, the maximum incorporation rate would be a function of the inhibitor dissociation rate. However, we previously determined for the wild-type that the maximum incorporation rate in the presence of saturating amounts of nonnucleoside inhibitors was entirely a consequence of turnover by the I·E·DNA complex (Spence et al., 1995). Because the parameters governing the polymerization mechanism of Y181C are similar to those for the wild-type RT, it can be argued that the slow rate of catalysis by the mutant I·E·DNA complex is due to catalysis by the inhibited E·-DNA complex as found for the wild-type enzyme.

The pre-steady-state studies that we have performed on Y181C indicate that Y181 does not play a critical role in the polymerization mechanism of RT and that replacement of this residue with cysteine will not attenuate replication of the virus. As we have described, Y181 is a major contributor to the interactions required to bind tightly and specifically a majority of the nonnucleoside inhibitors to HIV-1 RT. Unfortunately, the rapid mutation of Y181 upon prolonged use of nonnucleoside inhibitors with little consequence on the replication of the virus currently dampens the outlook for the potential use of nonnucleoside inhibitors in the struggle to fight AIDS. Recent efforts to inhibit the polymerization activity of RT have focused on convergent combination therapy using both nucleotide analogs and nonnucleoside inhibitors. The success of this therapy is dependent upon one class of inhibitors remaining sensitive against the RT resistant mutants that may develop from prolonged use of the other type of drug. We have provided a biochemical analysis of one of the most commonly isolated RT mutants resistant to nonnucleoside inhibitors: Y181C. Our conclusion that tight nucleotide binding still exists for Y181C (in the presence or absence of a nonnucleoside inhibitor) should increase interest in combination therapy, whereby a nucleotide analog may bind tightly to nonnucleoside resistant RT mutants, such as Y181C. The characteristics of both nucleotide analogs and nonnucleoside inhibitors may be utilized to form a tight-binding compound.

ACKNOWLEDGMENT

We sincerely thank Ulrike Immendoerfer and Dr. Roger Goody (Max Plank Institute) for providing the clones of the p66(Y181C) and p51(WT) subunits and Ulrike Immendoerfer for her advice in producing the p51(Y181C) mutation. Our appreciation is extended to Dr. Susan Gilbert (University of Pittsburgh) for helpful discussions and critical reading of the manuscript.

REFERENCES

Amann, E., & Brosius, J. (1985) *Gene 40*, 183.

Ausubel, F. M., Brent, R., Kingston, R. E., et al. (1992) *Current Protocols in Molecular Biology*, Green Publishing Associates and Wiley-Interscience, New York.

Baba, M., Tanaka, H., De Clercq, E., Pauwels, R., Balzarini, J., Schols, D., Nakashima, H., Perno, C.-F., Walker, R. T., & Miyasaka, T. (1989) *Biochem. Biophys. Res. Commun. 165*, 1375.

Balzarini, J., Karlsson, A., Perez-Perez, M. J., Vrang, L., Walbers, J., Zhang, H., Oberg, B., Vandamme, A. M., Camarasa, M. J., & De Clercq, E. (1993) *Virology 192*, 246.

Barre-Sinnoussi, F., Chremann, J. C., Rey, F., Nugmyre, M. T., Charmaret, S., Grhest, J., Dauguet, C., & Axler-Blin, C. (1983) *Science 220*, 868.

Condra, J. H., Emini, E. A., Gotlib, L., Graham, D. J., Schlabach, A. J., Wolfgang, J. A., Colonno, R. J., & Sardana, V. V. (1992) *Antimicrob. Agents Chemother. 36*, 1441.

De Clercq, E. (1994) *Biochem. Pharmacol. 47*, 155.

Debyser, Z., De Vreese, K., Knops-Gerrits, P. P., Baekelandt, V., Bhikhabhai, R., Strandberg, B., Pauwels, R., Anne, J., Desmyter, J., & De Clercq, E. (1993) *Mol. Pharmacol. 43*, 521.

Delarue, M., Poch, O., Tordo, N., Dino, M., & Argos, P. (1990) *Protein Eng. 3*, 461.

Ding, J., Das, K., Moereels, H., Koymans, L., Andries, K., Janssen, P. A. J., Hughes, S. H., & Arnold, E. A. (1995a) *Struct. Biol. 2*, 407.

Ding, J., Das, K., Tantillo, C., Zhang, W., Clark, A. D. J., Jessen, S., Lu, X., Hsiou, Y., Jacobo-Molina, A., Andries, K., Pauwels, R., Moereels, H., Koymans, L., Janssen, P. A. J., Smith, R. H. J., Koepke, M. K., Michejda, C. J., Hughes, S. H., & Arnold, E. A. (1995b) *Structure 3*, 365.

Dueweke, T. J., Kezdy, F. J., Waszak, G. A., Deibel, M. R., Jr., & Tarpley, W. G. (1992) *J. Biol. Chem. 267*, 27.

Esnouf, R., Ren, J., Ross, C., Jones, Y., Stammers, D., & Stuart, D. (1995) *Struct. Biol. 2*, 303.

Goldman, M. E., Nunberg, J. H., O'Brien, J. A., Quintero, J. C., Schleif, W. A., Freund, K. F., Gaul, S. L., Saari, W. S., Wai, J. S., Hoffman, J. M., Anderson, P. S., Hupe, D. J., Emini, E. A., & Stern, A. M. (1991) *Proc. Natl. Acad. Sci. U.S.A. 88*, 6863.

Goldman, M. E., O'Brien, J. A., Ruffing, T. L., Schleif, W. A., Sardana, V. V., Byrnes, V. W., Condra, J. H., Hoffman, J. M., & Emini, E. A. (1993) *Antimicrob. Agents Chemother. 37*, 947.

Hirsch, M. S., & D'Aquila, R. T. (1993) *New Engl. J. Med. 328*, 1686.

Hsieh, J. C., Zinnen, S., & Modrich, P. (1993) *J. Biol. Chem. 268*, 24607.

Johnson, K. A. (1986) *Methods Enzymol. 134*, 677.

Kati, W. M., Johnson, K. A., Jerva, L. F., & Anderson, K. S. (1992) *J. Biol. Chem. 267*, 25988.

Kohlstaedt, L. A., Wang, J., Friedman, J. M., Rice, P. A., & Steitz, T. A. (1992) *Science 256*, 1783.

Kruhoffer, M., Urbanke, C., & Grosse, F. (1993) *Nucleic Acids Res. 21*, 3943.

Larder, B. A., & Kemp, S. D. (1989) *Science 246*, 1155.

Larder, B. A., Darby, G., & Richman, D. D. (1989a) *Science 243*, 1731.

Larder, B. A., Kemp, S. D., & Purifoy, D. J. M. (1989b) *Proc. Natl. Acad. Sci. U.S.A. 86*, 4803.

Lightfoote, M. M., Coligan, J. E., Folks, T. M., Fauci, A. S., Martin, M. A., & Venkatesan, S. (1986) *J. Virol. 60*, 771.

Loya, S., Bakhanashvili, M., Tal, R., Hughes, S. H., Boyer, P. L., & Hizi, A. (1994) *AIDS Res. Hum. Retroviruses 10*, 939.

Maass, G., Immendoerfer, U., Koenig, B., Leser, U., Mueller, B., Goody, R., & Pfaff, E. (1993) *Antimicrob. Agents Chemother. 37*, 2612.

Maniatis, T., Fritsch, E. F., & Sambrook, J. (1989) in *Molecular Cloning: A Laboratory Manual*, Cold Spring Harbor Laboratory Press, Plainview, NY.

Mellors, J. W., Dutschman, G. E., Im, G. J., Tramontano, E., Winkler, S. R., & Cheng, Y. C. (1992) *Mol. Pharmacol. 41*, 446.

Mellors, J. W., Im, G. J., Tramontano, E., Winkler, S. R., Medina, D. J., Dutschman, G. E., Bazmi, H. Z., Piras, G., Gonzalez, C. J., & Cheng, Y. C. (1993) *Mol. Pharmacol. 43*, 11.

Merluzzi, V. J., Hargrave, K. D., Labadia, M., Grozinger, K., Skoog, M., Wu, J. C., Shih, C. K., Eckner, K., Hattox, S., Adams, J., Rosehthal, A. S., Faanes, R., Eckner, R. J., Koup, R. A., & Sullivan, J. L. (1990) *Science 250*, 1411.

Mitsuya, H., Yarchoan, R., & Broder, S. (1990) *Science 249*, 1533.

Muller, B., Restle, T., Weiss, S., Gautel, M., Sczakiel, G., & Goody, R. S. (1989) *J. Biol. Chem. 264*, 13975.

Nunberg, J. H., Schleif, W. A., Boots, E. J., O'Brien, J. A., Quintero, J. C., Hoffman, J. M., Emini, E. A., & Goldman, M. E. (1991) *J. Virol. 65*, 4887.

Patel, P. H., Jacobo-Molina, A., Ding, J., Tantillo, C., Clark, A. D., Raag, R., Nanni, R. G., Hughes, S. H., & Arnold, E. (1995) *Biochemistry 34*, 5351.

Pauwels, R., Andries, K., Desmyter, J., Schols, D., Kukla, M. J., Breslin, H. J., Raeymaeckers, A., Van Gelder, J., Woestenborghs, R., Heykants, J., Schellekens, K., Janssen, M. A. C., De Clercq, E., & Janssen, P. A. J. (1990) *Nature 343*, 470.

Pauwels, R., Andries, K., Debyser, Z., Van Daele, P., Schols, D., Stoffels, P., De Vreese, K., Woestenborghs, R., Vandamme, A. M., Janssen, C. G., Anne, J., Cauwenbergh, G., Desmyter, J., Heykants, J., Janssen, M. A. C., De Clercq, E., & Janssen, P. A. J. (1993) *Proc. Natl. Acad. Sci. U.S.A. 90*, 1711.

Pelletier, H., Sawaya, M. R., Kumar, A., Wilson, S., & Kraut, J. (1994) *Science 264*, 1891.

Popovic, M., Sarnghdharan, M. G., Read, E., & Gallo, R. C. (1984) *Science 224*, 497.

Reardon, J. E., & Miller, W. H. (1990) *J. Biol. Chem. 265*, 20302.

Ren, J., Esnouf, R., Garman, E., Somers, D., Ross, C., Kirby, I., Keeling, J., Darby, G., Jones, Y., Stuart, D., & Stammers, D. (1995) *Struct. Biol. 2*, 293.

Richman, D. D. (1993) *Antimicrob. Agents Chemother. 37*, 1207.

Richman, D., Shih, C. K., Lowy, I., Rose, J., Prodanovich, P., Goff, S., & Griffin, J. (1991) *Proc. Natl. Acad. Sci. U.S.A. 88*, 11241.

Richman, D. D., Havlir, D., Corbeil, J., Looney, D., Ignacio, C., Spector, S. A., Sullivan, J., Cheeseman, S., Barringer, K., Pauletti, D., Shih, C.-K., Myers, M., & Griffin, J. (1994) *J. Virol. 68*, 1660.

Rittinger, K., Divita, G., & Goody, R. S. (1995) *Proc. Natl. Acad. Sci. U.S.A. 92*, 8046.

Rodgers, D. W., Gamblin, S. J., Harris, B. A., Ray, S., Culp, J. S., Hellmig, B., Woolf, D. J., Debouck, C., & Harrison, S. C. (1995) *Proc. Natl. Acad. Sci. U.S.A. 92*, 1222.

Sardana, V. V., Emini, E. A., Gotlib, L., Graham, D. J., Lineberger, D. W., Long, W. J., Schlabach, A. J., Wolfgang, J. A., & Condra, J. H. (1992) *J. Biol. Chem. 267*, 17526.

Shih, C. K., Rose, J. M., Hansen, G. L., Wu, J. C., Bacolla, A., & Griffin, J. A. (1991) *Proc. Natl. Acad. Sci. U.S.A. 88*, 9878.

Spence, R. A., Kati, W. M., Anderson, K. S., & Johnson, K. A. (1995) *Science 267*, 988.

Steitz, T. A. (1993) *Curr. Opin. Struct. Biol. 3*, 31.

Tantillo, C., Ding, J., Jacobo-Molina, A., Nanni, R. G., Boyer, P. L., Hughes, S. H., Pauwels, R., Andries, K., Janssen, P. A., & Arnold, E. (1994) *J. Mol. Biol. 243*, 369.

Wu, J. C., Warren, T. C., Adams, J., Proudfoot, J., Skiles, J., Raghavan, P., Perry, C., Potocki, I., Farina, P. R., & Grob, P. M. (1991) *Biochemistry 30*, 2022.

BI952058+